7. *Appendix A*: Capabilities of the proposed control architecture

Remark 1. As a first comment, note that the *contact-lifting problem* (see Algorithm 2 in the manuscript) can be used to perform quasi-static stepping both on a flat ground and on an uneven terrain. This algorithm infact produces the CoM position $\overline{\boldsymbol{r}}_{CoM}$ and the contact forces $\overline{\boldsymbol{F}}_{\mathrm{C}}$, given the desired (pre-planned) contact positions $\boldsymbol{r}_{\mathrm{C}}^{\mathrm{des}}$, the related contact normals (not necessarily co-planar) $\boldsymbol{n}_{\mathrm{C}}^{\mathrm{des}}$ and the lifting contact/s. In order to highlight this feature, we reformulated the following paragraph in Section IV.C (please refer to the numbering of Sections of the resubmitted version of the manuscript):

> *- Contact lifting, see Algorithm 2: produces a single quasi-static pose, in terms of CoM position $\overline{\mathbf{r}}_{CoM}$ and the contact forces $\overline{\boldsymbol{F}}_{C}$, given the desired (pre-planned) contact positions $\boldsymbol{r}_{C}^{des}$, the related contact normals (not necessarily co-planar) $\boldsymbol{n}_{C}^{des}$ and the lifting contact/s. The force on the lifting contact/s $\mathbf{F}_{C,lift}$ is set to zero (6b), while the positions of the stance contacts $\mathbf{r}_{C,stance}$ are constrained to be equal to the desired value (6c). This algorithm can be applied iteratively to perform quasi-static stepping on flat or uneven terrains, once a set of planned contact positions and normals are provided.*

Remark 2. In order to show an example of the capability of the proposed *multi-contact planner* in addressing alternative scenarios involving different continuous environment descriptions, let us consider a 2-dimensional biped gap crossing task. For this 2-dimensional scenario $k = 2n_{\mathrm{C}}$ and the number of contact points n_{C} is equal to 2. Let $\boldsymbol{r}_{\mathrm{CoM}} \in \mathbb{R}^2$ be the position of the Center of Mass (CoM), while $\boldsymbol{F}_{\mathrm{C},i} \in \mathbb{R}^2$ and $\boldsymbol{r}_{\mathrm{C,i}} \in \mathbb{R}^2$ are the contact force and the related contact point at the i^{th} contact, for $i := \{1, 2\}$. Finally, let us require the CoM to move from the initial position $\boldsymbol{r}_{\mathrm{CoM}}^{\mathrm{start}} \in \mathbb{R}^2$ to the target position $\boldsymbol{r}_{\mathrm{CoM}}^{\mathrm{end}} \in \mathbb{R}^2$ in a prescribed number of steps n_{step}. In order to optimize the biped quasi-static pose at each step, the resulting set of decision variables is given by:

$$\boldsymbol{x} = \begin{bmatrix} \boldsymbol{r}_{\mathrm{CoM}}^{[1]} & \dots & \boldsymbol{r}_{\mathrm{CoM}}^{[n_{\mathrm{step}}]} & \boldsymbol{r}_{\mathrm{C,i}}^{[1]} & \dots & \boldsymbol{r}_{\mathrm{C,i}}^{[n_{\mathrm{step}}]} & \boldsymbol{F}_{\mathrm{C,i}}^{[1]} & \dots & \boldsymbol{F}_{\mathrm{C,i}}^{[n_{\mathrm{step}}]} \end{bmatrix}^T \in \mathbb{R}^{(2k+2)n_{\mathrm{step}}}$$

here superscript $[j]$ is used to denote the corresponding variable at the j-th step.
By combining the key components of the *multi-contact planner* module, i.e.: the robot centroidal statics, a continuous description of the environment $S_{\mathrm{C}}(\boldsymbol{r}_{\mathrm{C},i})$ and Coulomb friction cones $\mathcal{F}(\boldsymbol{F}_{\mathrm{C},i}, \boldsymbol{r}_{\mathrm{C},i}, \mu)$, the biped gap crossing task can be accomplished by solving the following nonlinear programming (NLP) problem:

$$\min_{\boldsymbol{x}} \sum_{j=1}^{n_{\mathrm{step}}} \|\boldsymbol{r}_{\mathrm{CoM}}^{[j]} - \boldsymbol{r}_{\mathrm{CoM}}^{\mathrm{end}}\|^2_{2,W_{CoM}} + \sum_{j=1}^{n_{\mathrm{step}}} \|\boldsymbol{F}_{\mathrm{C}}^{[j]}\|^2_{2,W_F} \tag{5a}$$

subject to

$$m\boldsymbol{g} + \boldsymbol{G}_{\mathrm{CD}}\boldsymbol{F}_{\mathrm{C}}^{[j]} = \boldsymbol{0} \quad \text{for} \quad j := \{1, \dots, n_{\mathrm{step}}\} \tag{5b}$$

$$\boldsymbol{r}_{\mathrm{C},i}^{[j]} \in S_{\mathrm{C}}(\boldsymbol{r}_{\mathrm{C},i}^{[j]}) \quad \text{for} \quad j := \{1, \dots, n_{\mathrm{step}}\} \tag{5c}$$

$$\{\boldsymbol{F}_{\mathrm{C},i}^{[j]}, \boldsymbol{r}_{\mathrm{C},i}^{[j]}\} \in \mathcal{F}(\boldsymbol{F}_{\mathrm{C},i}^{[j]}, \boldsymbol{r}_{\mathrm{C},i}^{[j]}, \mu) \quad \text{for} \quad j := \{1, \dots, n_{\mathrm{step}}\} \tag{5d}$$

$$\underline{\mathbf{r}}_{\mathrm{CoM}} \leq \boldsymbol{r}_{\mathrm{CoM}}^{[j]} \leq \overline{\mathbf{r}}_{\mathrm{CoM}} \quad \text{for} \quad j := \{1, \dots, n_{\mathrm{step}}\} \tag{5e}$$

$$\underline{\boldsymbol{\delta}} \leq \boldsymbol{r}_{\mathrm{CoM}}^{[j]} - \boldsymbol{r}_{\mathrm{C},i}^{[j]} \leq \overline{\boldsymbol{\delta}} \quad \text{for} \quad j := \{1, \dots, n_{\mathrm{step}}\} \tag{5f}$$

$$\boldsymbol{r}_{\mathrm{C,stance}}^{[j]} = \boldsymbol{r}_{\mathrm{C,stance}}^{[j+1]} \quad \text{for} \quad j := \{1, \dots, n_{\mathrm{step}} - 1\} \tag{5g}$$

Constraint (5b) accounts for the centroidal statics model, being:

$$
\boldsymbol{G}_{\text{CD}}\boldsymbol{F}_{\text{C}} = \begin{bmatrix} 1 & 0 & 1 & 0 \\ 0 & 1 & 0 & 1 \\ -(r_{\text{CoM}_y} - r_{\text{C},1_y}) & (r_{\text{CoM}_x} - r_{\text{C},1_x}) & -(r_{\text{CoM}_y} - r_{\text{C},2_y}) & (r_{\text{CoM}_x} - r_{\text{C},2_x}) \end{bmatrix} \begin{bmatrix} F_{\text{C},1_x} \\ F_{\text{C},1_y} \\ F_{\text{C},2_x} \\ F_{\text{C},2_y} \end{bmatrix}
$$

Constraint (5c) enforces that contact points belong to the environment, which for the case of the gap crossing task can be modeled through the following continuous function:

$$
S_{\text{C}}(\boldsymbol{r}_{\text{C},i}) : r_{\text{C,i}_y} + \text{atan}\Big(k\ (r_{\text{C,i}_x} - \underline{r}_{\text{gap}_x})\Big) - \text{atan}\Big(k\ (r_{\text{C,i}_x} - \overline{r}_{\text{gap}_x})\Big) = 0
$$

where $\underline{r}_{\text{gap}_x},\ \overline{r}_{\text{gap}_x} \in \mathbb{R}$ are the gap lower and upper bound, respectively, along the x-axis, while $k \in \mathbb{R}$ is a coefficient which determines the sharpness of the gap corners.
Constraint (5d) accounts for Coulomb friction cones, while constraint (5e) accounts for bound on the CoM position. The initial and target CoM position, $\boldsymbol{r}_{\text{CoM}}^{\text{start}}$ and $\boldsymbol{r}_{\text{CoM}}^{\text{end}}$, respectively, are enforced as follows:

$$
\begin{aligned}
&\text{if}\ \ j = 1 :\ \underline{\mathbf{r}}_{\text{CoM}} = \overline{\mathbf{r}}_{\text{CoM}} = \boldsymbol{r}_{\text{CoM}}^{\text{start}} \\
&\text{if}\ \ j = n_{\text{step}} :\ \underline{\mathbf{r}}_{\text{CoM}} = \overline{\mathbf{r}}_{\text{CoM}} = \boldsymbol{r}_{\text{CoM}}^{\text{end}}
\end{aligned}
$$

The reachable work-space is approximated by means of the box constraint in (5f), while (5g) constraints the contact position for the stance foot at each step.

This analysis has been performed using the CasADi software package, for the following choice of parameters:

$$
\begin{gathered}
n_{\text{step}} = 5,\ m = 50\ kg, k = 10^6,\ \mu = 0.5, \\
\boldsymbol{r}_{\text{CoM}}^{\text{start}} = \begin{bmatrix} 0.5 & 1 \end{bmatrix}^T \boldsymbol{r}_{\text{CoM}}^{\text{end}} = \begin{bmatrix} 7.5 & 1 \end{bmatrix}^T,\ \begin{bmatrix} \underline{r}_{\text{gap}_x} & \overline{r}_{\text{gap}_x} \end{bmatrix} = \begin{bmatrix} 3 & 4 \end{bmatrix}
\end{gathered}
$$

and compared to the flat ground case, i.e. $S_{\text{C}}(\boldsymbol{r}_{\text{C},i}) : r_{\text{C,i}_y} = 0$.
As it can be noticed from Fig. I, the proposed NLP problem produces a sequence of quasi-static poses that allows to reach the CoM target position, while accomplishing the gap crossing task, see Fig. 1(b). Note that, compared to the flat ground case in Fig. 1(a), the contact position $\boldsymbol{r}_{\text{C},2}^{[2]}$ at the 2-nd step (red dot) is now placed in the proximity of the gap corner in order to allow the crossing within the work-space limits.

Based on this analysis, we decided to add the following paragraph in Section IV.C (please refer to the numbering of Sections of the resubmitted version of the manuscript):

> *Note that, in order to produce a sequence of n_s quasi-static poses, Algorithm 1 can be modified by extending the decision variable vector as follows:*
>
> $$\boldsymbol{x} = \begin{bmatrix} \boldsymbol{r}_{CoM}^{[1]} & \dots & \boldsymbol{r}_{CoM}^{[n_s]} & \boldsymbol{r}_{C,i}^{[1]} & \dots & \boldsymbol{r}_{C,i}^{[n_s]} & \boldsymbol{F}_{C,i}^{[1]} & \dots & \boldsymbol{F}_{C,i}^{[n_s]} \end{bmatrix}^T$$
>
> *and by constraining the positions of the stance contacts at each step. This eventually allows for quasi-static locomotion in unstructured environments, e.g. a gap crossing task, assuming a suitable continuous function for the environment is provided, at the expense of computational complexity due to the increased problem dimension.*

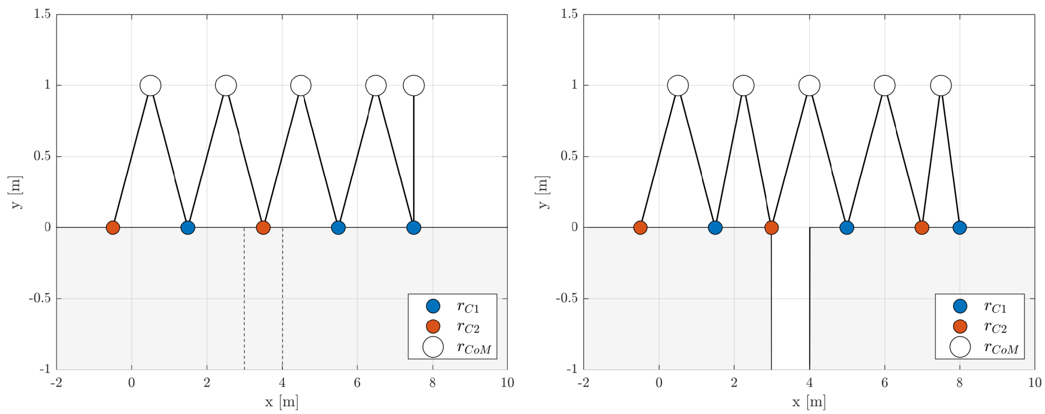

(a) Bipedal locomotion on a flat ground.

(b) Bipedal gap crossing task (flat ground with a $1m$ gap).

Figure I: 2-dimensional bipedal locomotion task.

Remark 3. As highlighted by the gap crossing example, note that a generic continuous function describing the environment complexity is compatible with the proposed *multi-contact planner*.

In particular, we propose to employ *superquadric* functions as a convenient description of perpendicular surfaces, like the ground/wall environment involved in the pushing task, but also narrow passages or corridors.

As far as the authors' knowledge, Winkler et al. "*Gait and trajectory optimization for legged systems through phase-based end-effector parameterization*" is the only work in the field of motion planning for legged robots that deals with *hard* contact models based on a continuous description of the environment. Alternatively, *soft* contact models can be found e.g. in Mordatch et al. "*Discovery of complex behaviors through contact-invariant optimization*" and in Neunert et al. "*Whole-body nonlinear model predictive control through contacts for quadrupeds*". These approaches show good performance but are known to be prone to physical inconsistencies, e.g. surface penetrations and contact forces that never completely vanish.

Compared to Winkler et al., which employs smooth height-maps to combine different environment surfaces, superquadrics are more effective in modelling vertical walls, whereas Winkler et al. would require to consider tilted planes. For the sake of fairness, note that this advantage comes at the expense of curved corners among the planes.

Note also that, while superquadrics have been recently employed in robot grasping, see Vezzani et al. "*A grasping approach based on superquadric models*", their adoption in motion planning for legged robots is a novel contribution of this paper.

In order to highlight these features, we rephrased the following paragraph in Section IV.A as follows (please refer to the numbering of Sections of the resubmitted version of the manuscript):

> *A. Continuous Environment Description: Superquadric*
>
> *Representing the environment with separate convex-hulls can be a useful simplification in contacts planning approaches, although it inherently requires mixed-integer optimization [10], [11]. In agreement with [16], we here consider a hard contact model for the environment based on a unique continuous function. This choice allows for continuous optimization, and consequently speeds up calculations compared to mixed-integer programming. Soft contact models can be alternatively employed, see [12], [14], although they are prone to produce physical inconsistencies, e.g. surface penetrations with contacts.*

In particular, we propose to employ superquadric functions as a convenient description of perpendicular surfaces, e.g. the ground/wall environment involved in the pushing task, but also narrow passages or corridors. While superquadrics have been recently employed in robot grasping, see [29], their adoption in motion planning for legged robots is novel. Note that, compared to [16], which employs smooth height-maps to combine different environment surfaces, superquadrics are more effective in modelling vertical walls, whereas [16] would require to consider tilted planes. This, on the other end, comes at the expense of curved corners.

Remark 4. As a final remark, we would like to stress the generality of the proposed control architecture in handling different robotic platforms as bipeds. A sequence of snapshots from a Gazebo simulation of COMAN+ balancing with two feet on a wall are shown in Fig. II. These results are also illustrated in a video available at the following link: `https://youtu.be/rqP1ANbdu7I`. Fig. III finally shows a snapshot taken from a preliminary experimental trial.

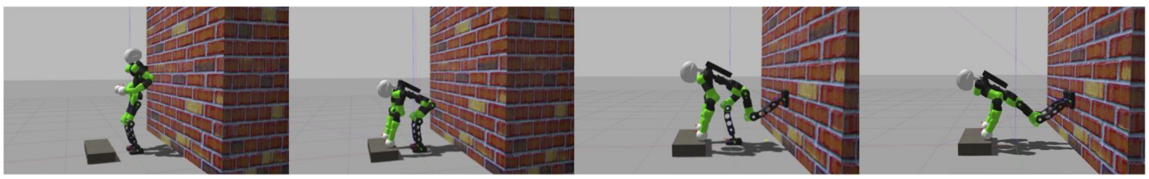

Figure II: Snapshots from a Gazebo simulations of the humanoid COMAN+ balancing with two feet touching a wall.

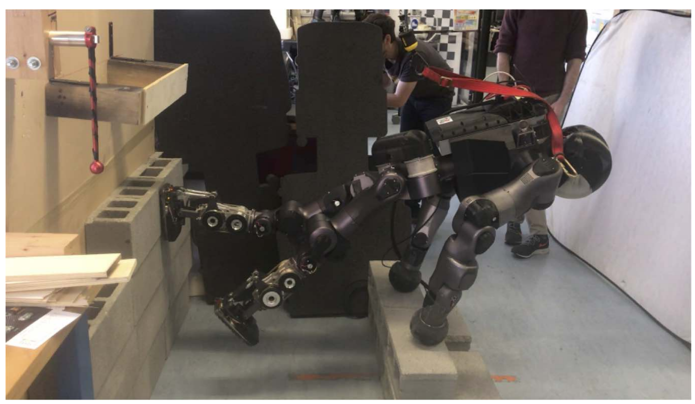

Figure III: Snapshots from a preliminary experiment trial on COMAN+.